Journal of Scientific Computing manuscript No.
(will be inserted by the editor)

A Positive Definite Limiter for Advection Problems

James Kent

Received: date / Accepted: date

Abstract Advection schemes are important in many branches of computational fluid dynamics. They are used for tracer transport in atmospheric models, where the tracer mixing ratios must remain positive. Many advection schemes employ monotonic limiters, however these can reduce the accuracy of the schemes for smooth data. In this article a commonly used monotonic limiter is modified to make it positive definite (but not strictly monotonic). Testing in multiple dimensions shows that there is improved accuracy over the monotonic limiter, while no negative values are produced.

Keywords Tracer · Transport · Monotonicity · Finite-Difference

Mathematics Subject Classification (2010) 65M06 · 65M08 · 35Q86

1 Introduction

Accurate advection schemes are an important part of any atmospheric model, as they are used for the transport of tracers and in the solution of conservation laws. Many finite-volume and finite-difference methods employ limiters to ensure monotonicity. However, these limiters can be overly diffusive for smooth data, and therefore reduce the formal order-of-accuracy of the underlying scheme [5]. Although monotonicity is often desired in a model, an essential property of an advection scheme for tracer transport is positivity. Negative values for a tracer mixing ratio or density are unphysical and can have adverse effects in physics parameterizations. A positive-definite advection scheme ensures that quantities cannot take physically unrealistic negative values. Previous work has shown how some monotonic limiters can be reduced to being positive definite (see, for example, [12,8]). In this article it is shown how the monotonic limiters of [7] (for one-dimension) and [13] (for multi-dimensions) can be relaxed, with detailed steps,

J. Kent
Computing and Mathematics, University of South Wales, Pontypridd, CF37 1DL, UK
Tel.: +441443 482269
E-mail: james.kent@southwales.ac.uk

to make positive definite limiters. These limiters are choosen because they have been used across many climate modelling applications [1,9,11]. Results from the numerical testing in this article highlight the advantages and disadvantages of using the positive definite form of these limiters for advection problems.

2 One-Dimensional Positive Definite Limiter

First we consider the one-dimensional advection equation for tracer density,

$$\frac{\partial \rho q}{\partial t} + \frac{\partial u \rho q}{\partial x} = 0, \tag{1}$$

where q is the tracer mixing ratio, ρ is the density, and u is the velocity. This can be solved in flux form as

$$(\rho q)_i^{n+1} = \rho_i^n q_i^n - \frac{\Delta t}{\Delta x}\left(\hat{s}_{i+1/2}\hat{q}_{i+1/2} - \hat{s}_{i-1/2}\hat{q}_{i-1/2}\right) \tag{2}$$

where $s = u\rho$, n is the temporal index, i is the spatial index, Δt is the time step, and Δx is the spatial step (assumed constant in this case). The circumflex indicates the value of a quantity at a grid cell edge. Assuming that the mass fluxes, $\hat{s} = \hat{u}\hat{\rho}$, are known, then a basic scheme, which is not monotonic or positive-definite, is used to compute $\hat{q}$, and this is denoted $\hat{q}^{\text{basic}}$. The limiter is then applied to $\hat{q}$.

First we review the Universal Limiter for one-dimensional flow [7], using the notation of [13]. For each cell edge we let $C = |u|\Delta t/\Delta x$ represent the Courant number, and $\tilde{C} = C\hat{\rho}/\rho_i^n$ the Courant number at a cell edge modified by the density of that cell. For this demonstration we assume a velocity from left to right, and so we define subscript L for quantities on the left edge of the cell (the inflow to the cell) and subscript R for quantities on the right edge of the cell (the outflow from the cell).

The steps are as follows:

(i) Define inflow bounds:

$$(\hat{q}_L^{in})_{\min} = \min(q_{i-1}^n, q_i^n), \qquad (\hat{q}_L^{in})_{\max} = \max(q_{i-1}^n, q_i^n). \tag{3}$$

(ii) Adjust these values using the basic scheme:

$$\hat{q}_L'' = \max[\min(\hat{q}_L^{\text{basic}}, (\hat{q}_L^{in})_{\max}), (\hat{q}_L^{in})_{\min}]. \tag{4}$$

(iii) Define minimum and maximum values at the next time step:

$$(q_i^{n+1})_{\min} = (\hat{q}_L^{in})_{\min}, \qquad (q_i^{n+1})_{\max} = (\hat{q}_L^{in})_{\max}. \tag{5}$$

(iv) Calculate outflow bounds:

$$(\hat{q}_i^{\text{out}})_{\max} = \frac{q_i^n + \tilde{C}_L(\hat{q}_L^{in})_{\min} - (q_i^{n+1})_{\min}(1 + \tilde{C}_L - \tilde{C}_R)}{\tilde{C}_R}$$

$$(\hat{q}_i^{\text{out}})_{\min} = \frac{q_i^n + \tilde{C}_L(\hat{q}_L^{in})_{\max} - (q_i^{n+1})_{\max}(1 + \tilde{C}_L - \tilde{C}_R)}{\tilde{C}_R}$$

(v) Adjust edge values:

$$\hat{q}_R = \max[\min(\hat{q}''_R, (\hat{q}_i^{\text{out}})_{\max}), (\hat{q}_i^{\text{out}})_{\min}] \tag{6}$$

The positive definite version of this limiter adjusts the monotonic limiter given above to allow overshoots and undershoots but remain positive definite. The minimum inflow bounds are set to zero while the maximum inflow bounds are unused. The minimum value at step $n+1$ is set to zero, as is the minimum outflow bound. The maximum outflow bound is calculated as per step (iv) above, and the edge value calculated as step (v). For simplicity, the steps for the positive definite limiter are shown below:

(I) Calculate inflow bounds using the basic scheme and zero:

$$\hat{q}''_L = \max(\hat{q}_L^{\text{basic}}, 0) \tag{7}$$

(II) Adjust face values:

$$\hat{q}_R = \max\left[\min\left(\hat{q}''_R, \frac{q_i^n}{\tilde{C}_R}\right), 0\right] \tag{8}$$

To evaluate this positive definite limiter we run a number of numerical tests. The positive definite limiter (denoted PD) is compared against the basic scheme, and the basic scheme with the limiter of [7] (denoted LIM). The domain is of size 1 and is periodic. We run tests with three sets of initial conditions: a smooth sine wave, $q = 1/2\sin(2\pi x) + 1$; the cosine squared bell defined by [15]; and a step function centred at $x = 1/2$ with width $1/2$. In each case $\rho = 1$ and $u = 1$ are constants, and the time step is chosen such that the Courant number is $C = 0.1$. The normalised ℓ_2 error norms are calculated on the grid with 64 grid points, and for the sine wave the empirical convergence rate is calculated using the error norms from the 64 and 128 grid point grids [3]. The basic schemes are second, third- and fourth-order versions of the Lax-Wendroff scheme [6,14,2].

Table 1 Normalized ℓ_2 error norms for schemes on the grid with 64 grid points for the sine wave, the cosine bell, and the step function initial conditions. Also show is the empirical convergence rate for the sine wave.

	Sine Wave		Cosine Bell	Step
Order	$\ell_2(q)$	Rate	$\ell_2(q)$	$\ell_2(q)$
2nd	2.3×10^{-3}	2.0	0.46	0.28
2nd LIM	4.0×10^{-3}	1.7	0.24	0.20
2nd PD	2.3×10^{-3}	2.0	0.33	0.25
3rd	1.1×10^{-4}	3.0	0.12	0.17
3rd LIM	4.0×10^{-4}	2.2	0.11	0.17
2nd PD	1.1×10^{-4}	3.0	0.09	0.17
4th	4.4×10^{-6}	4.0	5.4×10^{-2}	0.18
4th LIM	6.2×10^{-4}	2.0	5.0×10^{-2}	0.14
4th PD	4.4×10^{-6}	4.0	3.5×10^{-2}	0.16

The results for the one-dimensional testing are shown in Table 1. For each order-of-accuracy for the sine wave the schemes with the positive definite limiter have the same error norms and convergence rates as the basic scheme. These error

norms and convergence rates are an improvement on when the full limiter is used. For non-smooth data the full limiter produces lower error norms than the basic scheme. The positive definite limiter has similar magnitude error norms to the full limiter for these initial conditions. Figure 1 plots the solution for the step function initial conditions for the third-order basic scheme. The basic scheme produces over- and undershoots, while the full limiter keeps the tracer within the original maximum and minimum. The positive definite limiter ensures that the minimum of the solution is zero, however it allows overshoots. This demonstrates that the positive definite limiter is not monotonic.

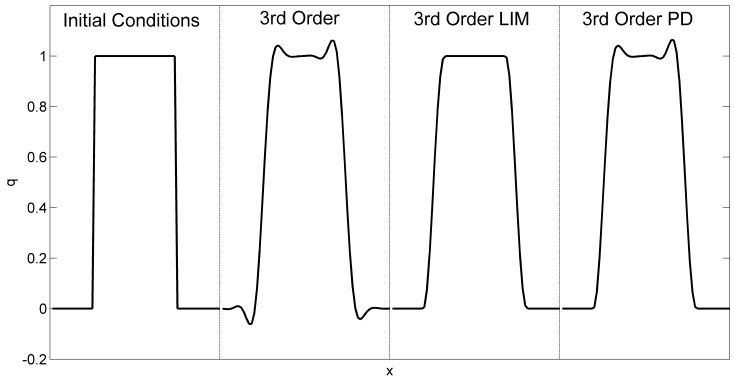

Fig. 1 Solution of the one-dimensional advection equation for the step function using the 3rd order basic scheme on the 64 grid point grid.

3 Multi-Dimensional Positive Definite Limiter

We now consider two-dimensional flow on a square grid, although this limiter can be extended to multiple dimensions and any shape grid cell. The tracer density equation is now

$$\frac{\partial \rho q}{\partial t} + \frac{\partial u \rho q}{\partial x} + \frac{\partial v \rho q}{\partial x} = 0, \tag{9}$$

which can be solved in flux form as

$$\begin{aligned}(\rho q)_{ij}^{n+1} = \rho_{ij}^n q_{ij}^n \; &- \frac{\Delta t}{\Delta x}\left(\hat{r}_{i+1/2j}\hat{q}_{i+1/2j} - \hat{r}_{i-1/2j}\hat{q}_{i-1/2j}\right) \\ &- \frac{\Delta t}{\Delta y}\left(\hat{s}_{ij+1/2}\hat{q}_{ij+1/2} - \hat{s}_{ij-1/2}\hat{q}_{ij-1/2}\right).\end{aligned} \tag{10}$$

Here $r = u\rho$ and $s = v\rho$, n is the temporal index, but now u and v are the velocities in the x and y directions, with i and j the corresponding spatial indices, and Δx and Δy the corresponding spatial steps (again assumed constant in this case).

First we review the limiter of [13] for multi-dimensional flow. As for the one dimensional case we assume that the mass fluxes are known and that the superscript 'basic' indicates that the cell edge value has been calculated using a

non-monotonic (or non-positive definite) scheme. Again, C denotes the absolute value of the Courant number at a cell edge, and $\tilde{C}$ denotes the modified Courant number. We use subscript I for quantities on the inflow edge of the cell, and subscript O for quantities on the outflow edge of the cell. The superscript 'up' indicates values from an upwind area. The steps are as follows:

(i) Define inflow bounds at each inflow face I:

$$(\hat{q}_I^{in})_{\min} = \min(q_{\min}^{up}, q_{ij}^n), \qquad (\hat{q}_I^{in})_{\max} = \max(q_{\max}^{up}, q_{ij}^n) \tag{11}$$

(ii) Adjust these values using the basic scheme:

$$\hat{q}_I'' = \max[\min(\hat{q}_I^{\text{basic}}, (\hat{q}_I^{in})_{\max}), (\hat{q}_I^{in})_{\min}] \tag{12}$$

(iii) Define minimum and maximum values at the next time step:

$$(q_{ij}^{n+1})_{\min} = \min_I(\hat{q}_I^{in})_{\min}, \qquad (q_{ij}^{n+1})_{\max} = \max_I(\hat{q}_I^{in})_{\max} \tag{13}$$

(iv) Calculate outflow bounds:

$$(\hat{q}_{ij}^{\text{out}})_{\max} = \frac{q_{ij}^n + \sum_I \tilde{C}_I(\hat{q}_I^{in})_{\min} - (q_{ij}^{n+1})_{\min}(1 + \sum_I \tilde{C}_I - \sum_O \tilde{C}_O)}{\sum_O \tilde{C}_O}$$

$$(\hat{q}_{ij}^{\text{out}})_{\min} = \frac{q_{ij}^n + \sum_I \tilde{C}_I(\hat{q}_I^{in})_{\max} - (q_{ij}^{n+1})_{\max}(1 + \sum_I \tilde{C}_I - \sum_O \tilde{C}_O)}{\sum_O \tilde{C}_O}$$

(v) Adjust face values for each outflow face O:

$$\hat{q}_O = \max[\min(\hat{q}_O'', (\hat{q}_{ij}^{\text{out}})_{\max}), (\hat{q}_{ij}^{\text{out}})_{\min}] \tag{14}$$

As for the one-dimensional case, the positive definite limiter adjusts the monotonic limiter given above to allow overshoots and undershoots but remain positive definite. The minimum inflow and outflow bounds, as well as the minimum value at step $n+1$ are all set to zero. The maximum outflow bound is calculated as per step (iv) above, and the edge value calculated as step (v). For simplicity, the steps for the positive definite limiter are shown below. Step I must be done for all inflow edges and step II for all outflow edges:

(I) Calculate inflow bounds using the basic scheme:

$$\hat{q}_I'' = \max(\hat{q}_I^{\text{basic}}, 0) \tag{15}$$

(II) Adjust face values:

$$\hat{q}_O = \max\left[\min\left(\hat{q}_O'', \frac{q_{ij}^n}{\sum_O \tilde{C}_O}\right), 0\right] \tag{16}$$

To test the positive definite limiter in two-dimensions we use a Cartesian form of the deformation test described by [10]. The velocity is non-divergent and is prescribed as

$$u(x, y, t) = 2\sin^2(\pi x')\sin(2\pi y)\cos(\pi t) + 1, \tag{17}$$
$$v(x, y, t) = -2\sin^2(\pi y)\sin(2\pi x')\cos(\pi t), \tag{18}$$

where $x' = x - \Delta t$ is used to translate the velocities. The $\cos(\pi t)$ term reverses the flow at the halfway point of the simulation, allowing the initial conditions to be used as the analytical solution. Three sets of initial tracer mixing ratios are used: the first is a smooth sine wave

$$q = 0.5 + 0.5\sin(2\pi x)\sin(2\pi y); \tag{19}$$

the second is a pair of exponential hills (where $r = 100$)

$$q = \exp(-r(x - 0.25)^2 - r(x - 0.5)^2) + \exp(-r(x - 0.75)^2 - r(x - 0.5)^2); \tag{20}$$

and the third is a set of discontinuous steps where, for $d_1 = 1/4$ and $d_2 = 3/4$,

$$q = \{\, 1 \quad \text{if } (x - d_i) < 1/10 \text{ and } (y - 1/2) < 1/10, 0 \quad \text{else.} \tag{21}$$

The density $\rho = 1$ is a constant. The domain is doubly periodic of size 1, and the test is performed on a uniform grid of 64 grid points in both directions. The time step $\Delta t = 1/320$ is chosen to ensure that the maximum Courant number is less than one. The basic schemes are second, third- and fourth-order versions of the multi-dimensional Lax-Wendroff scheme.

Table 2 Normalized ℓ_2 error norms for schemes on the grid with 64 grid points in each direction for the exponential hills and the step function initial conditions, and the minimum and maximum values at the end of the simulation for the step function. The empirical convergence rate is calculated using error norms on the 128 grid point grid.

Order	Sine $\ell_2(q)$	Rate	Hills $\ell_2(q)$	Rate	Step $\ell_2(q)$	Step min	Step max
2nd	0.064	1.92	0.410	1.11	0.547	-0.356	1.284
2nd LIM	0.055	1.71	0.280	1.05	0.484	0	0.884
2nd PD	0.065	1.92	0.314	0.94	0.496	0	1.199
3rd	0.013	2.85	0.194	1.87	0.421	-0.080	1.085
3rd LIM	0.014	2.83	0.195	1.79	0.432	0	0.953
3rd PD	0.013	2.85	0.183	1.80	0.421	0	1.077
4th	0.003	3.50	0.125	2.92	0.377	-0.263	1.297
4th LIM	0.009	2.33	0.115	1.99	0.375	0	0.977
4th PD	0.003	3.48	0.099	2.60	0.376	0	1.319

The results for the two-dimensional testing are shown in Table 2. For the smooth sine wave the results for the positive definite limiter are similar to those of the basic scheme (for each order). For the other initial conditions, the addition of the positive definite limiter or the full limiter generally results in lower error norms than the basic scheme. The schemes with the positive definite limiter have error norms of a similar magnitude to the corresponding fully limited schemes. For the step functions, the minimum value when the positive definite limiter is used is zero but the maximum value slightly exceeds the initial value. This overshoot is

reduced when a diffusive basic scheme, such as the third-order scheme, is used. The solutions for the step function initial conditions for the third-order basic scheme are shown in Figure 2.

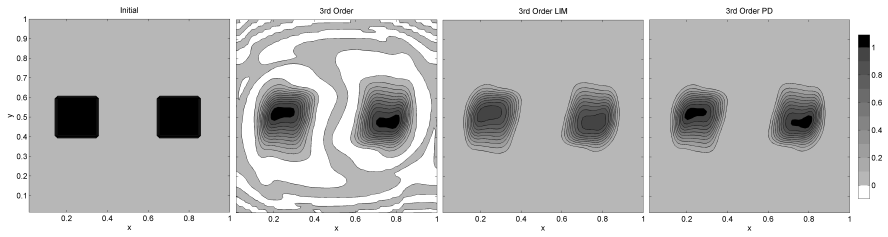

Fig. 2 Solution of the two-dimensional advection equation for the step function using the 3rd order basic scheme on the 64×64 grid. The left plot shows the initial conditions (and analytical solution).

The preservation of pre-existing correlations between tracer species is important for atmospheric chemistry models [4]. To test the ability of the positive definite limiter to preserve such correlations, the deformational flow is used with 3 related tracer mixing ratios: q_1 is the exponential hills; $q_2 = 1 - q_1$ provides a linear correlation; $q_3 = 1 - q_1^2$ provides a non-linear correlation.

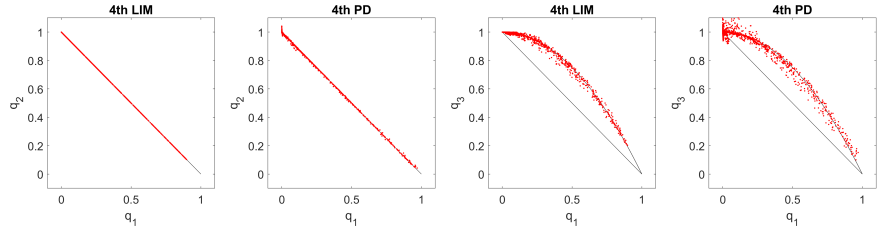

Fig. 3 Correlation preservation using the full limiter and the positive definite limiter with the 4th order scheme. The left two plots compare a linear relationship (q_1 and q_2), and the right two plots compare a non-linear relationship (q_1 and q_3).

Figure 3 shows scatter plots of q_1 against q_2, and q_1 against q_3 at the half way point of the deformation simulation using the 4th order scheme with the full limiter and the positive definite limiter. The full limiter maintains the linear correlation throughout the simulation, whereas the positive definite limiter is unable to maintain the linear correlation when q_1 is close to zero. The full limiter performs well for the non-linear correlation, with only small non-physical overshoots. The positive definite limiter performs worse than the full limiter, with large non-physical overshoots, again near where q_1 is close to zero. These results hold for the 2nd and 3rd order basic schemes.

In addition to the deformational testing shown above, a divergent deformational test is used to demonstrate the positive definite limiter for divergent flows. The initial tracer is that of the discontinuous steps, the denisity is initially $\rho = 1$,

and the velocity is given as (where x' is the translated coordinate)

$$u(x, y, t) = -\sin(\pi x')\sin(\pi x')\sin(2\pi y)\cos^2(2\pi y)\cos(\pi t) + 1, \tag{22}$$

$$v(x, y, t) = \frac{1}{2}\sin(2\pi x')\cos^3(2\pi y)\cos(\pi t). \tag{23}$$

The minimum value of the tracer is recorded at each time step. Results shows that both the positive definite and full limiter (for all orders-of-accuracy) maintain a minimum of zero (to machine precision), demonstrating that this limiter is positive definite even for divergent flows.

4 Conclusions

In some applications, such as atmospheric tracer transport, a positive definite limiter may be more suitable than a fully monotonic limiter for solving the advection equation. We have shown how to modify the limiters of [7] and [13] to become positive definite (but not monotonic) limiters for multidimensional flow. Using these new positive definite limiters it is possible to achieve the order-of-accuracy of the underlying basic scheme. Results for one-dimensional and two-dimensional advection tests show that the application of the positive definite limiter produces similar error norms to the full monotonic limiter, and confirm that no unphysical negative values are produced, for non-divergent or divergent flow. However, the positive definite limiter is unable to maintain a linear correlation between tracer species.

Acknowledgements I would like to thank two anonymous reviewers for their comments that greatly improved the manuscript.

References

1. Chawla, A., Spindler, D. M. and Tolman, H. L. 2013. Validation of a thirty year wave hindcast using the Climate Forecast System Reanalysis winds. *Ocean Modelling*, **70**, 189-206.
2. Holdaway, D. and Kent, J. 2015. Assessing the tangent linear behavior of common tracer transport schemes and their use in a linearized atmospheric general circulation model. *Tellus A*, **67**, 27895. doi:http://dx.doi.org/10.3402/tellusa.v67.27895
3. Holdaway, D., Thuburn, J. and Wood, N. 2008. On the relation between order of accuracy, convergence rate and spectral slope for linear numerical methods applied to multiscale problems. *International Journal For Numerical Methods in Fluids*, **56**, 1297-1303.
4. Lauritzen, P. H. and Thuburn, J. 2012. Evaluating advection/transport schemes using interrelated tracers, scatter plots and numericalmixing diagnostics. *Q. J. R. Meteorol. Soc.*, **138**, 906-918.
5. Lauritzen, P. H., Ullrich, P. A., Jablonowski, C., Bosler, P. A., Calhoun, D., Conley, A. J., Enomoto, T., Dong, L., Dubey, S., Guba, O., Hansen, A. B., Kaas, E., Kent, J., Lamarque, J. F., Prather, M. J., Reinert, D., Shashkin, V. V., Skamarock, W. C., Sorensen, B., Taylor, M. A., and Tolstykh, M. A. 2014. A Standard Test Case Suite For Two-Dimensional Linear Transport on the Sphere: Results From a Collection of State-of-the-Art Schemes. *Geosci. Model Dev.*, **5**, (2012) 887-901.
6. Lax, P. D. and Wendroff, B. 1960. Systems of conservation laws. *Commun. Pure Appl. Math.*, **13**, 217-237.
7. Leonard, B. P. 1991. The ULTIMATE conservative difference scheme applied to unsteady one-dimensional advection. *Comput. Methods Appl. Mech. Eng.*, **88**. 17-74.

8. Lin, S. J. and Rood, R. B. 1996. Multidimensional Flux-Form Semi-Lagrangian Transport Schemes. *Mon. Weather Rev.*, **124**, 2046-2070.
9. Miura, H. 2007. An Upwind-Biased Conservative Advection Scheme for Spherical Hexagonal–Pentagonal Grids. *Mon. Weather Rev.*, **135**, 4038-4044.
10. Nair, R. D. and Lauritzen, P. H. 2010. A class of deformational flow test cases for linear transport problems on the sphere. *J. Comput. Phys.*, **229**, 8868-8887.
11. Ringler, T. D., Thuburn, J., Klemp, J. B. and Skamarock, W. C. 2010. A unified approach to energy conservation and potential vorticity dynamics for arbitrarily-structured C-grids. *J. Comput. Phys.*, **229**, 3065-3090.
12. Smolarkiewicz, P. K. 1983. A simple positive definite advection scheme with small implicit diffusion. *Mon. Weather Rev.*, **111**, 479-486.
13. Thuburn, J. 1996. Multidimensional flux-limited advection schemes. *J. Comput. Phys.*, **23**, 74-83.
14. Tremback, C. J., Powell, J., Cotton, W. R. and Pielke, R. A. 1987. The forward-in-time upstream advection scheme: extension to higher orders. *Mon. Weather Rev.*, **115**, 540-555.
15. Zerroukat, M., Wood, N. and Staniforth, A. 2005. The parabolic spline method (PSM) for conservative transport problems. *Int. J. Num. Meth. Fluids*, **51, 1297-1318.**